# INVERSE ENERGY CASCADE IN 2D TURBULENCE: EXPERIMENTAL STUDY

J. PARET AND P. TABELING
*Laboratoire de Physique Statistique, Ecole Normale Supérieure*
*24 rue Lhomond, 75231 Paris Cedex 5, France.*

## 1. Introduction

Thirty years ago, Kraichnan [1] conjectured that the twin constraints of energy and enstrophy conservation for inviscid two-dimensional flows should impose the existence of two different inertial ranges for 2D turbulence forced at a given scale: an enstrophy transferring range extending from the input scale towards the viscous scale (the direct enstrophy cascade) and an energy transferring range extending from the input scale towards large scale, known as the inverse energy cascade. Kraichnan proposed that the latter range should display a Kolmogorov type scaling:

$$E(k) = C_k \varepsilon^{2/3} k^{-5/3}$$

as long as this scaling range does not extend to scales comparable to that of the fluid domain. When the cascade reaches the box size, he conjectured that the flow should experience a kind of Bose-Einstein condensation with a pile-up of kinetic energy in the lowest accessible mode. Since then, a number of numerical simulations have confirmed these conjectures [2, 3] but, aside from the early observations by Sommeria [4], there was no experimental evidence supporting them.

We provide here the results of an extensive experimental study of the two-dimensional inverse energy cascade which show that Kraichnan's conjectures were basically correct. Moreover, we investigate intermittency effects and the role of coherent structures in the inverse cascade regime and show that the inverse cascade is non-intermittent with quasi-gaussian statistics. Finally, the study of relative dispersion of pairs of passive particles shows that it is ruled by Richardson's law, $R^2 \sim t^3$.

The experimental set-up we use has been described in a number of papers (see Ref. [5] for a detailed description). It is made of a 15 cm $\times$ 15 cm



*U. Frisch (ed.), Advances in Turbulence VII*, 445–448.

PVC cell filled with two thin layers of electrolyte in a stable configuration (the heavier underlying the lighter). Permanents magnets are placed below the cell and the interaction of their vertical magnetic field with an electric current driven from one side of the cell to the other produces Laplace forces which drive the flow. The latter is visualized by latex particles placed at the free surface, recorded on a video tape and further processed by standard PIV techniques which allow us to obtain the complete velocity fields at any time. In the present experiments, we use total fluid depths of 5.5 mm (inverse cascade) and 7.5 mm (condensate), the injection scale $l_i$ is 1.5 cm and the injection Reynolds number (based on the injection scale and the root-mean-square velocity) is around 100.

## 2. Inverse energy cascade

When the bottom friction (which is the main dissipation mechanism in this system) is not too low, we have found that, after a short transient, a stationary regime is achieved and that the flow is homogeneous and isotropic in this regime, with an energy spectrum (Fig. 1(a)) displaying a scaling range with scaling exponent very close to $-5/3$ [6]. Moreover, the Kolmogorov constant was determined to be $C_K \sim 6.5$, a value consistent with numerical estimates. Although the scaling range we observe is not very wide, it is well defined and it is then natural to wonder whether there exist any intermittency corrections as it is the case for 3D turbulence. We have performed this analysis using ensemble averaging over 5 experiments, each having a duration of about 40 turn-over times. Although the absolute scaling exponents for the structure functions are not well defined due to the modest size of our inertial range, relative exponents for longitudinal structure functions, determined using ESS, can be measured and they are equal, within experimental accuracy, to their Kolmogorov values, $\zeta_p = p/3$ (Fig. 2(a)). Moreover, normalized even-order moments $H_{2n} = S_{2n}/(S_2)^n$, either longitudinal or transverse, are almost undistinguishable from their gaussian values up to order 12. These results show that there is no intermittency in the inverse cascade range. We have also determined the distribution of vortex sizes (Fig. 2(b)). Vortices are characterized by thresholding the vorticity fields at $\pm 1.5$ their rms value and keeping the region with vorticity levels above the threshold. We find that the distribution of vortex sizes has a peak for a size corresponding to the injection scale and then exponentially decreases at larger sizes. This observation shows that the role of coherent structures in the inverse cascade dynamics is probably not the naive one, involving the formation of larger and larger vortices through merging events. We have indeed observed that merging events are rare and that the dynamics are rather governed by the aggregation of same sign vortices into

large recirculation regions.

## 3. Bose-Einstein condensation

By increasing the total fluid depth, we are able to decrease the bottom friction. When this friction is low enough, the condensation process is observed: the energy accumulates into the lowest accessible mode and the energy spectrum displays a sharp bump at this wave-number (Fig. 1(b)), with a scaling consistent with a $k^{-3}$ energy spectrum although it is not developped enough to draw a definite conclusion. The flow displays a mean global rotation with weak superimposed fluctuations even if the forcing injects an approximately zero net circulation. Moreover, this mean rotation is organized around a central vortex with very high vorticity, an observation in agreement with the vortex intensification process observed numerically by Smith and Yakhot [3].

## 4. Richardson's law

Finally, we studied the relative dispersion of pairs of particles initially close to each other. This is done by numerically integrating the equations of motion for passive particles using the experimentally measured velocity fields. This technique allows to easily determine a large number of trajectories, which is necessary in order for the statistical analysis to make sense. We typically compute several tens of thousand trajectories and the mean squared separation between particles is found to follow Richardson's law $R^2 \sim t^3$ (Fig. 3).

## 5. Conclusion

This comprehensive experimental study of the inverse energy cascade shows that, depending on the external friction at large scales, two different stationary regimes can be achieved. The inverse cascade regime, with $-5/3$ scaling, appears to be non-intermittent and to be driven by an aggregation mechanism of same sign vortices. Moreover, for this regime, relative dispersion of pairs of particles is in agreement with Richardson's law. These results tend to confirm the picture of the inverse cascade advocated by Kraichnan. Moreover, the fact that the properties of the inverse cascade can be essentially derived from dimensional analysis leads us to wonder whether it could be accessible to a full theoretical treatment.

## References


1. Kraichnan, R.H. (1967): Inertial ranges in two-dimensional turbulence, *Phys. Fluids* **10**, 1417–1423.
2. Maltrud, M.E. and Vallis, G.K. (1991): Energy spectra and coherent structures in forced two-dimensional and beta-plane turbulence, *J. Fluid Mech.* **228**, 321–342.
3. Smith, L.M. and Yakhot, V. (1994): Finite-size effects in forced two-dimensional turbulence, *J. Fluid Mech.* **274**, 115–138.
4. Sommeria, J. (1986): Experimental study of the two-dimensional inverse energy cascade in a square box, *J. Fluid Mech.* **170**, 139–168.
5. Cardoso, O., Marteau, D. and Tabeling, P. (1994): Quantitative experimental study of the free decay of quasi-two-dimensional turbulence, *Phys. Rev. E* **49**, 454–461.
6. Paret, J. and Tabeling, P. (1997): Experimental observation of the two-dimensional inverse energy cascade, *Phys. Rev. Lett.* **79**, 4162–4165.


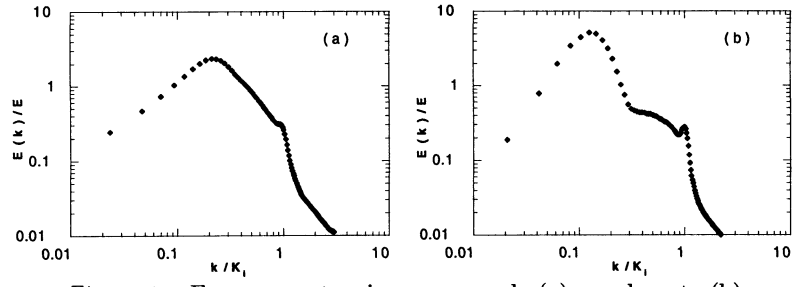


*Figure 1.* Energy spectra: inverse cascade (a), condensate (b).

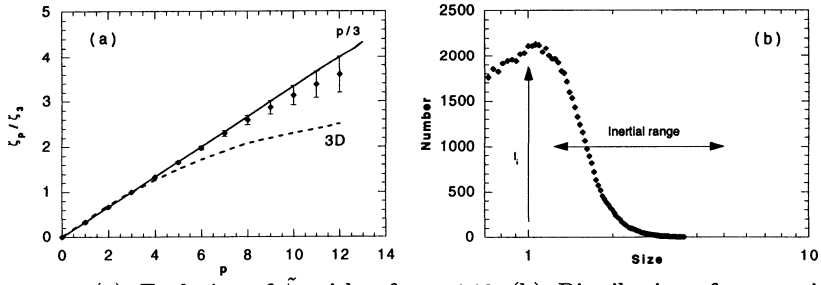


*Figure 2.* (a): Evolution of $\tilde{\zeta_p}$ with $p$ for $p \leq 12$. (b): Distribution of vortex sizes.

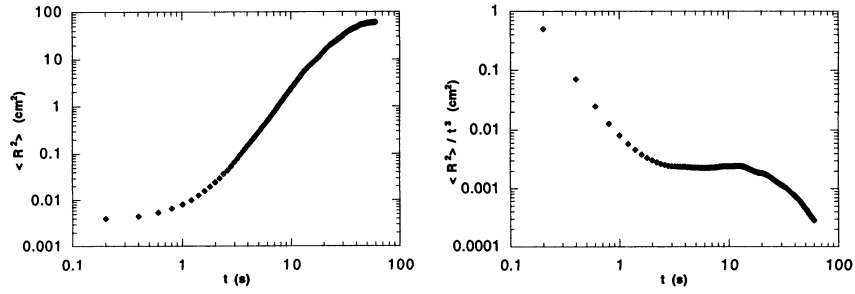


*Figure 3.* Evolution of the mean squared separation $\langle R^2 \rangle$. (a): $\langle R^2 \rangle$ vs. $t$, (b): $\langle R^2 \rangle / t^3$ vs. $t$.